Published in final edited form as:
Hepatology. 2012 March ; 55(3): 833–845. doi:10.1002/hep.24736.

AKT and N-Ras co-activation in the mouse liver promotes rapid carcinogenesis via mTORC1, FOXM1/SKP2, and c-Myc pathways

Coral Ho[1,†], **Chunmei Wang**[1,†], **Sandra Mattu**[2], **Giulia Destefanis**[2], **Sara Ladu**[3], **Salvatore Delogu**[2], **Julia Armbruster**[2], **Lingling Fan**[1], **Susie A. Lee**[1], **Lijie Jiang**[1], **Frank Dombrowski**[2], **Matthias Evert**[2], **Xin Chen**[1,4,5], and **Diego F. Calvisi**[2,5]

[1]Department of Bioengineering and Therapeutic Sciences, University of California, San Francisco, USA

[2]Institut für Pathologie, Ernst-Moritz-Arndt-Universität, Greifswald, Germany

[3]Department of Medicine and Aging, Section of Epidemiology and Public Health, University of Chieti, Chieti, Italy.

[4]Liver Center, University of California, San Francisco, USA

Abstract

Activation of v-akt murine thymoma viral oncogene homolog (AKT) and Ras pathways is often implicated in carcinogenesis. However, the oncogenic cooperation between these two cascades in relationship to hepatocellular carcinoma (HCC) development remains undetermined. To investigate this issue, we generated a mouse model characterized by combined overexpression of activated forms of AKT and neuroblastoma Ras viral oncogene homolog (N-Ras) protooncogenes in the liver via hydrodynamic gene transfer. The molecular mechanisms underlying crosstalk between AKT and N-Ras were assessed in the mouse model and further evaluated in human and murine HCC cell lines. We found that co-expression of AKT and N-Ras resulted in a dramatic acceleration of liver tumor development when compared with mice overexpressing AKT alone, whereas N-Ras alone did not lead to tumor formation. At the cellular level, concomitant upregulation of AKT and N-Ras resulted in increased proliferation and microvascularization when compared with AKT injected mice. Mechanistic studies suggested that accelerated hepatocarcinogenesis driven by AKT and N-Ras resulted from a strong activation of mammalian target of rapamycin complex 1 (mTORC1). Furthermore, elevated expression of FOXM1/SKP2 and c-Myc also contributed to rapid tumor growth in AKT/Ras mice, yet via mTORC1-independent mechanisms. The biological effects of co-activation of AKT and N-Ras were then

[5]**Correspondence:** Xin Chen, UCSF, 513 Parnassus Ave., San Francisco, CA 94143, U.S.A. Tel: (415) 502-6526; Fax: (415) 502-4322; xin.chen@ucsf.edu; or Diego F. Calvisi, Institut für Pathologie, Ernst-Moritz-Arndt-Universität, Friedrich-Löffler-Str. 23e, 17489 Greifswald, Germany. Telephone: 0049 3834 865719; Fax: 0049 3834 865704; diego.calvisi@uni-greifswald.de. .
[†]Coral Ho and Chunmei Wang contributed equally to this work.
Coral Ho: hoc@pharmacy.ucsf.edu
Chunmei Wang: Chunmei.Wang@ucsf.edu
Sandra Mattu: mattu.sandra@yahoo.it
Giulia Destefanis: destefanisgiulia@yahoo.it
Sara Ladu: saraladu@gmail.com
Salvatore Delogu: buiertola@libero.it
Julia Armbruster: juliarmbruster@gmx.de
Lingling Fan: Lingling.Fan@ucsf.edu
Susie A. Lee: ms_susiq@yahoo.com
Lijie Jiang: Lijie.Jiang@ucsf.edu
Frank Dombrowski: frank.dombrowski@uni-greifswald.de
Matthias Evert: matthias.evert@uni-greifswald.de
Xin Chen: xin.chen@ucsf.edu
Diego F. Calvisi: diego.calvisi@uni-greifswald.de

recapitulated *in vitro* using HCC cell lines, which supports the functional significance of mTORC1, FOXM1/SKP2 and c-Myc signaling cascades in mediating AKT and N-Ras induced liver tumor development.

Conclusion—Our data demonstrate the *in vivo* crosstalk between the AKT and Ras pathways in promoting liver tumor development, and the pivotal role of mTORC1-dependent and independent pathways in mediating AKT and Ras induced hepatocarcinogenesis.

Keywords

hepatocellular carcinoma; MAPK; mTOR; hydrodynamic injection

Hepatocellular carcinoma (HCC) is the fifth most common type of malignancy and the third cause of tumor death worldwide.[1] Treatment options for HCC are limited and generally ineffective.[1] Surgical resection or liver transplantation is the only curative treatment, but most of the patients are ineligible for surgery due to the late stage of the disease at the time of diagnosis.[1] Sorafenib, a multi-kinase inhibitor, is the only chemotherapeutic drug available for the treatment of unresectable HCC.[2] However, it has limited efficacy in improving survival of HCC patients, most likely due to the activation of alternative pathways promoting the survival of tumor cells.[2] Thus, the investigation of the molecular pathogenesis of HCC is necessary for the development of new targeted therapies against this deadly disease.

Deregulation of multiple signaling cascades has been found to be implicated in human hepatocarcinogenesis. Among them, unrestrained activation of the Ras/mitogen-activated protein kinase (MAPK) and v-akt murine thymoma viral oncogene homolog (AKT)/ mammalian target of rapamycin (mTOR) pathways seem to play a major role both in liver malignant transformation and tumor progression.[3-6]

Ras proteins are members of a family of small guanosine triphosphate (GTP)-regulated molecular switches for signaling pathways that modulate cell growth, survival, and migration.[7] Once activated, Ras induces the protein kinase activity of RAF kinase. Raf phosphorylates and activates MAPK kinase kinase (MEK), which subsequently phosphorylates and activates extracellular signal-regulated kinase (ERK), ultimately leading to up-regulation of downstream targets.[7]

Similarly, the AKT/mTOR cascade influences growth, survival, metabolism, and migration of numerous cell types, including liver cancer cells.[8,9] mTOR is the catalytic subunit of two distinct complexes, called mTOR complex 1 (mTORC1) and mTORC2. Two accessory proteins, regulatory-associated protein of mTOR (RAPTOR) and rapamycin-insensitive companion of mTOR (RICTOR), define mTORC1 and mTORC2, respectively.[8,9] mTORC1 mediates cell growth by stimulating protein synthesis via phosphorylation of p70 ribosomal protein S6 kinase (p70 S6K) and eukaryotic initiation factor 4E binding protein 1 (4E-BP1). p70 S6K phosphorylates the ribosomal protein S6 (RPS6), resulting in increased translation of mRNAs containing a 5′ oligopyrimidine tract, whereas phosphorylation of 4E-BP1 by mTOR relieves inhibition on the initiation factor eIF4E, resulting in more efficient cap-dependent translation.[8,9] mTORC2 activates instead a growing number of distinct effectors, including Akt and serum- and glucocorticoid-regulated kinase 1 (SGK1).[9]

Despite the importance of Ras and AKT/mTOR signaling cascades in hepatocarcinogenesis, their functional interaction has not been examined in liver cancer, especially *in vivo*. To study the crosstalk between these two oncogenic pathways, we developed a novel mouse model of liver cancer that overexpresses the activated forms of AKT and N-Ras genes. Here, we show that co-expression of activated AKT and N-Ras promotes accelerated

hepatocarcinogenesis when compared with overexpression of either AKT or N-Ras alone, providing *in vivo* evidence of their cooperation in liver cancer. Furthermore, our findings imply that mTORC1-dependent and –independent mechanisms are responsible for AKT/Ras driven hepatocarcinogenesis.

Materials and Methods

Hydrodynamic Injection and Mouse Monitoring

Wild-type FVB/N mice were obtained from Charles River (Wilmington, MA). The constructs used in the study and experiments showing long term expression of genes via hydrodynamic injection are showed in Supplementary Fig. 1. Hydrodynamic injection was performed as described.[10-12] In brief, 10μg of the plasmids encoding myr-AKT1 and/or N-RasV12 along with sleeping beauty transposase in a ratio of 25:1 were diluted in 2 mL saline (0.9% NaCl), filtered though 0.22 μm filter, and injected into the lateral tail vein of 6 to 8-week-old FVB/N mice in 5 to 7 seconds. Mice were housed, fed, and monitored in accordance with protocols approved by the committee for animal research at the University of California, San Francisco.

Histology, Immunohistochemistry, and Immunofluorescence

Liver lesions were assessed by two board-certified pathologists (M.E. and F.D.) in accordance with the criteria by Frith et al.[13] Immunohistochemistry was performed as described.[12] For immunofluorescence staining, frozen sections were incubated with the rat monoclonal anti-CD34 primary antibody (1:200, eBioscience, San Diego, CA), followed by goat anti-rat conjugated to Alexa 594 (1:500, Invitrogen, Carlsbad, MA) secondary antibody. Slides were mounted with Vectashield mounting medium containing DAPI (Vector Laboratories, Burlingame, CA). Images were acquired using the Olympus BX51 fluorescence microscope (Olympus America Inc., Center Valley, PA).

Cell Lines

Transfection of *in vitro* growing cell lines with siRNAs and cDNAs with specific inhibitors were performed as described in Supporting Information.

Immunoblotting and Immunoprecipitation

Murine hepatic tissues were processed as reported in Supporting Information. Nitrocellulose membranes were probed with specific primary antibodies (Supplementary Table 1).

Statistical Analysis

Tukey-Kramer test was used to evaluate statistical significance. Values of $P < 0.05$ were considered significant. Data are expressed as means ± SD.

See Supporting Information for more detailed descriptions of Materials and Methods.

RESULTS

Concomitant Expression of Myristylated-AKT1 and N-RasV12 in the Mouse Liver Rapidly Induces Liver Tumors

To study the genetic and biochemical interactions between the Ras/MAPK and AKT/mTOR cascades *in vivo*, we stably expressed activated forms of human neuroblastoma Ras viral oncogene homolog (N-Ras; N-RasV12)[11] and human AKT1 (myristylated AKT1 or myr-AKT1, with C-terminal HA tag)[12] in the mouse liver via hydrodynamic injection. Consistent with previous studies,[14] overexpression of N-RasV12 alone did not induce histological

abnormalities in the mouse liver. Overexpression of myr-AKT1 (which will be referred to as AKT mouse) induced instead lipogenesis and hepatocyte proliferation that resulted in liver hepatocellular adenomas ~12 weeks post injection, and eventually HCC ~ 6 months post injection, as previously shown.[12] Co-expression of myr-AKT1 and N-RasV12 (which will be referred to as AKT/Ras mouse) resulted in a massive abdomen enlargement within 4 weeks after injection (Fig. 1A) and mice became moribund, requiring to be euthanized by 6 weeks (Fig. 1B). Liver size was significantly augmented as early as 2 to 3 weeks after injection, and it continued to enlarge throughout the time course (Fig. 1C). Also, the color of liver changed, becoming more inhomogeneous, spotty and paler than in normal controls (data not shown). Four weeks after injection, several nodular lesions emerged from the liver parenchyma, finally occupying most of its surface (Fig. 1D).

Histological examination of the liver tissue after one week showed already many altered hepatocytes. The latter had a massively enlarged clear cytoplasm, owing to an increase in glycogen and fat storage (Fig. 2A), and were morphologically indistinguishable from preneoplastic hepatocytes from AKT injected mice, which were described previously in detail.[12] Altered hepatocytes were often located in zone 3 of the liver acinus and occupied ~20-30% of the parenchyma. Two weeks after injection, the lesions maintained the clear-cell phenotype and occupied up to 40% of the parenchymal liver volume. Three weeks after injection, the altered tissue occupied up to two-thirds of the hepatic parenchyma (Fig. 2B). The same extent of liver volume was occupied by preneoplastic lesions not before 12 weeks after injection in AKT mice. Lesions still consisted mainly of clear-cell hepatocytes; however, the first tumor-like nodules (each measuring less than 1 mm in diameter) developed (Fig. 2B,C). The nodules showed an expansive growth compressing the adjacent cells and consisted of basophilic hepatocytes with a higher nuclear/cytoplasmic ratio and enlarged nuclei; single mitotic figures were visible, both in preneoplastic (Fig. 2A) and neoplastic lesions (not shown). Four weeks after injection, the overall amount of preneoplastic tissue did not increase significantly, but individual lesions progress into tumors in all examined animals (Fig. 2D). Tumors were of mixed cellularity, measuring up to 2 mm in diameter; signs of malignancy such as severe cytologic atypia, necrosis, macrotrabecular growth pattern, vascular invasion, or infiltrative growth, were absent at this time-point. A trabecular hepatocellular differentiation was the predominant phenotype, although tumors with small foci of ductular differentiation, hepatocellular tumors with a significant portion of ductules, and pure cholangiocellular tumors were also detected. Five weeks after injection, preneoplastic lesions and tumors occupied up to 90% of the liver parenchyma (Fig. 2E,F). Several frankly malignant tumors, mostly pure hepatocellular carcinomas and, to a lesser degree, mixed hepatocellular/cholangiocellular or pure cholangiocellular carcinomas developed (Fig. 2E,F). No distant metastases were detected in AKT/Ras mice at any time point.

To confirm that preneoplastic and neoplastic lesions were indeed induced by the ectopically injected oncogenes, we performed immunohistochemistry on AKT/Ras lesions by using an anti-HA-tag, an anti-activated/phosphorylated AKT, and an anti-human N-Ras antibody (Supplementary Fig. 2). As expected, preneoplastic lesions (Supplementary Fig. 2A-C) and tumors (Supplementary Fig. 2D-F) but not the normal liver tissue showed strong expression of HA-tag, activated AKT, and human N-Ras proteins. Importantly, the immunolabeling for HA-tag, activated AKT, and human N-Ras co-localized in preneoplastic lesions (Supplementary Fig. 2A-C) and homogeneously stained the tumors in their entirety (Supplementary Figure 2D-F), implying the concomitant activation of AKT and N-Ras in the same cell clusters and the crucial role of these proteins both in the early and late stages of hepatocarcinogenesis.

In summary, we established a novel mouse model for HCC and demonstrated that co-expression of activated AKT and N-Ras results in accelerated hepatocarcinogenesis, providing, for the first time, *in vivo* evidence of cooperation between these two signaling cascades in liver cancer.

Co-expression of AKT1 and N-Ras Increases Proliferation and Angiogenesis of HCC Cells

To address the cellular mechanisms responsible for accelerated hepatocarcinogenesis, we compared proliferation, apoptosis, and angiogenesis indices in preneoplastic and neoplastic lesions from AKT and AKT/Ras mice (Fig. 3). Proliferation index was significantly higher in AKT/Ras preneoplastic lesions and tumors when compared with AKT corresponding lesions (Fig. 3A; Supplementary Fig. 3A,B). The most pronounced angiogenesis, as assessed by microvessel density count, was detected in AKT/Ras tumors (Fig. 3C), whereas no difference were observed in preneoplastic lesions from AKT and AKT/Ras mice. The increased angiogenesis in AKT/Ras liver tumors was further confirmed via CD34 immunofluorescent staining (Supplementary Fig. 4). As concerns apoptosis, co-expression of AKT and N-Ras did not provide additional survival advantages effects when compared with AKT mice (Fig. 3B; Supplementary Fig. 3C,D).

Altogether, the data indicate that overexpression of N-Ras further stimulates proliferation and angiogenesis of altered hepatocytes driven by AKT but has no additional effects on apoptosis.

Co-expression of AKT and N-Ras Promotes Strong Activation of the mTORC1 Pathway

To elucidate the molecular mechanisms underlying the rapid tumor progression in AKT/Ras injected mice, we assayed the key signaling pathways downstream of AKT and Ras in wild-type livers and preneoplastic and neoplastic liver lesions from AKT and AKT/Ras mice by western blot analysis and immunohistochemistry (Fig. 4, 5, and Supplementary Fig. 5).

For Ras/MAPK cascade, we found that levels of human N-Ras (total and membranous) and activated N-Ras (N-Ras-GTP) were induced only in AKT/Ras livers. Also, activated/phosphorylated forms of RAF-1, ERK1/2, and c-JUN were highest in preneoplastic and neoplastic lesions from AKT/Ras mice. No differences were detected in the levels of activated H-Ras and Ki-Ras (total and activated; Fig. 4A; Supplementary Fig. 5) and in other Ras downstream effectors (p38MAPK, JNK) in wild-type, AKT, and AKT/Ras livers (not shown). Interestingly, immunohistochemistry for activated/phosphorylated ERK1/2 revealed the presence of a peculiar cell subpopulation in AKT/Ras preneoplastic lesions that was not present in AKT corresponding lesions (not shown). These cells displayed strong immunoreactivity for activated ERK1/2, high nuclear to cytoplasmic ratio, low lipid and glycogen storage in the cytoplasm, and high proliferation rate (Fig. 5A,B). Additionally, the cells positive for activated/phosphorylated ERK1/2 were often grouped together (Fig. 5B). AKT/Ras tumors were comprised in their entirety of this cell subpopulation (Fig. 5C), indicating that the latter cells possess growth advantages over the other cell clones. Importantly, cells positive for p-ERK1/2 staining were present only at the tumor stage in the AKT mice (not shown), suggesting that activation of ERK proteins is closely related to the malignant transformation of preneoplastic lesions driven by AKT.

For AKT/mTOR pathway, levels of activated AKT were equivalent in liver lesions from AKT and AKT/Ras mice and higher than in wild-type mice, whereas activation of mTOR was most elevated in AKT/Ras mice (Fig. 4B; Supplementary Fig. 5). Next, we assessed the levels of the members of mTORC1 and mTORC2 cascades. mTORC1 downstream effectors in protein translation (activated/phosphorylated p70 S6K and inactivated/phosphorylated 4E-BP1), angiogenesis (HIF-1α, VEGF-α), and apoptosis (MCL-1) were mostly upregulated

in AKT/Ras preneoplastic and neoplastic lesions, intermediate in AKT mice, and lowest in wild-type mice (Fig. 4B). However, the proteins responsible for the lipogenic phenotype, including FASN, ACAC, and SCD1, whose induction mainly depends on mTORC1 activation,[12] were equally upregulated in AKT and AKT/Ras preneoplastic lesions, but decreased at tumor stage in AKT/Ras mice (Fig. 4B; Supplementary Fig. 5). This finding suggests that *de novo* lipogenesis plays a role mainly in the early stages of AKT/Ras-driven tumor development, rather then in cancer progression. A similar upregulation of the mTORC2 targets, phosphorylated AKT and SGK1, was detected in AKT and AKT/Ras mice when compared with wild-type mice. Thus, the cooperation of N-Ras and AKT results in increased activity of mTORC1 rather than mTORC2 in the mouse liver. Since the Ras/MAPK pathway has been found to induce mTORC1 activation via phosphorylation/inactivation of tuberin (TSC2) at its serine 664 residue,[15] we assessed whether the same mechanism applies to liver cancer (Fig. 4*C*; Supplementary Fig. 5). Importantly, we found a strong induction of TSC2 phosphorylation at serine 664, which was paralleled by increased ERK-TSC2 complexes, reduction of TSC1-TSC2 complexes, and upregulation of RHEB in AKT/Ras lesions but not in AKT or wild-type livers. Higher levels than in wild-type livers, but no differences in TSC2 phosphorylation levels at serine 939 (that is targeted by AKT)[16] and in the phosphorylation/inactivation of PRAS40 (whose phosphorylation by AKT relieves PRAS40 inhibition of mTORC1)[17] between the two mouse models were observed (Fig. 4*C*; Supplementary Fig. 6). Also, we did not detect any difference in the three mice groups both in the expression of the SF2/ASF splicing factor, which promotes mTORC1 upregulation,[18] and in the levels of p90RSK-Raptor complexes, a sign of p90RSK-mediated activation of mTORC1 (Fig. 4C; Supplementary Fig. 6).[19] Expression patterns of some of the proteins tested by western blot were also confirmed via immunohistochemistry (Fig. 5D-F).

The role of AKT and N-Ras overexpression on *in vitro* cell growth was further investigated. A primary cell line (indicated as AKT/Ras cell line) was isolated from liver tumors induced by AKT/Ras co-injection. Simultaneous suppression of AKT and N-Ras resulted in a strong growth restraint and decrease of VEGF-α medium secretion in the AKT/Ras cell line when compared with silencing of either AKT or N-Ras alone (Fig. 6A,C), whereas no synergistic effect on apoptosis was detected (Fig. 6B). At the molecular level, suppression of AKT and Ras was accompanied by downregulation of Ras/MAPK, mTORC1 and mTORC2 cascades (Supplementary Fig. 7A). Equivalent results were obtained when AKT and N-Ras were silenced in human SNU-389 HCC cells (expressing high levels of N-Ras and AKT; not shown). On the other hand, combined overexpression of myr-AKT1 and N-RasV12 in the human HCC HLF cell line (expressing low levels of AKT and N-Ras) resulted in acceleration of cell growth and VEGF-α medium secretion (Fig. 6D,F), but not of apoptosis (Fig. 6E). Overexpression of AKT and Ras triggered upregulation of Ras/MAPK, mTORC1 and mTORC2 pathways (Supplementary Fig. 7B). Furthermore, suppression of MEK1, the upstream inducer of ERK, but not of MEK2 and AKT reduced the levels of phosphorylated/inactivated TSC2 at serine 664 and RHEB and augmented the complexes between TSC1 and TSC2 in the AKT/Ras cell line (Supplementary Fig. 8A). Conversely, only overexpression of MEK1 led to upregulation of TSC2 serine 664 phosphorylation and RHEB and downregulation of TSC1-TSC2 complexes in HLF cells (Supplementary Fig. 8B).

These findings indicate the crucial role of Ras/MEK1/MAPK pathway in amplifying the activation of mTORC1 driven by AKT.

Activation of FOXM1 and c-Myc Contributes to Unrestrained Proliferation in AKT/Ras induced HCC

Since increased proliferation is a major feature distinguishing AKT/Ras from AKT lesions, we determined the levels of cell cycle proteins and cell cycle inhibitors in the tumor samples

by western blot (Fig. 7A-C). Strikingly, we found that the forkhead box M1 (FOXM1) transcription factor and its targets responsible for cell cycle progression (PLK1, CDC25B, Aurora B, Cyclin B1)[20] and encoding the SCF ubiquitin ligase degradation complex (SKP2, CKS1)[20] were all predominantly upregulated in AKT/Ras preneoplastic and neoplastic lesions (Fig. 7A). As a consequence of the hyperactivation of the SCF complex, levels of cell cycle inhibitors targeted by SKP2-CKS1-dependent degradation (p27, p57, RASSF1A, and DUSP1)[21-23] were lowest in AKT/Ras lesions (Fig. 7B). In accordance with this finding, induction of phosphorylation of p27, p57, RASSF1A, and DUSP1 that primes these proteins for proteolysis[21-23] was highest in AKT/Ras mice (Fig. 7B). In addition, we found a remarkable upregulation of c-Myc and its target Odc predominantly in preneoplastic and neoplastic AKT/Ras lesions (Fig. 7C). Since it has been shown that Ras and AKT can induce upregulation of c-Myc by phosphorylating and promoting the degradation of MAD1,[24] we determined the levels of total and phosphorylated/inactivated MAD1 in the sample collection. Notably, we found that total MAD1 levels were lowest and phosphorylated MAD1 levels were highest in AKT/Ras mice (Fig. 7C), confirming the previous findings in HeLa cells.[24]

The functional consequences of AKT and N-Ras overexpression on FOXM1 and c-Myc cascades were further investigated *in vitro*. Concomitant suppression of AKT and N-Ras in the AKT/Ras cell line was accompanied by downregulation of FOXM1 and its targets as well as by suppression of c-Myc expression and upregulation of MAD1 (Fig. 7D). Equivalent results were obtained when AKT and N-Ras were silenced in human SNU-389 HCC cells (not shown). On the other hand, combined overexpression of AKT and N-Ras in HLF cells triggered upregulation of FOXM1 and its effectors, as well as upregulation of c-Myc and downregulation of MAD1 (Fig. 7E). In the same cell line, induction of FOXM1 targets but not of c-Myc was dramatically inhibited when combined overexpression of AKT and N-Ras was paralleled by FOXM1 silencing (not shown).

Due to the strong induction of the mTORC1 cascade in the AKT/Ras model, we determined whether upregulation of FOXM1 or c-Myc was dependent on mTORC1. However, silencing of the mTORC1 component RAPTOR in the AKT/Ras cell lines did not result in suppression of FOXM1 and c-Myc (Fig. 8A). Similarly, overexpression of AKT and Ras led to FOXM1 and c-Myc upregulation that was not suppressed by concomitant silencing of RAPTOR in HLF cells (Fig. 8B).

Next, we investigated the role of mTORC1, FOXM1/SKP2 and c-Myc pathways in mediating AKT and N-Ras induced HCC cell proliferation. For this purpose, we silenced RAPTOR, FOXM1 and c-Myc genes either alone or in combination in AKT/Ras HCC cell line via siRNA. As expected, silencing of each pathway alone led to decreased cell proliferation. However, concomitant suppression of Raptor, FOXM1, and c-Myc resulted in a complete suppression of cell growth in the AKT/Ras cell line (Fig. 8C).

Taken together, the present data indicate that mTORC1, FOXM1/SKP2 and c-Myc signalling cascades all significantly contribute to the cell growth properties of AKT and Ras. Nevertheless, activation of FOXM1/SKP2 and c-Myc pathways is independent of mTOR in this mouse model.

AKT and Ras Concomitant Overexpression Downregulates Ras/MAPK Inhibitors Leading to Strong Ras Activity

An interesting finding of the *in vitr*o studies was that N-Ras and ERK activated levels were most profoundly modulated when both AKT and N-Ras where either suppressed or overexpressed (Supplementary Fig. 7). In particular, the data indicate that AKT activation might further amplify the activation of the Ras/MAPK cascade. Since a previous report

indicates that AKT suppresses Ras activity via RAF-1 phosphorylation at serine 259,[25] we determined the latter parameter in our mouse collection (Supplementary Fig. 9). No differences were detected in the levels of phosphorylated/inactivated RAF-1 among wild-type, AKT, and AKT/Ras livers, indicating that AKT upregulation does not suppress the Ras/MAPK pathway in AKT and AKT/Ras mouse models. To unveil the mechanism(s) whereby AKT and Ras crosstalk further promotes activation of the Ras/MAPK pathway, we assessed the levels of known Ras and ERK inhibitors in the mouse collection. Strikingly, RASAL1, DAB2IP, NORE1A, RKIP, and SPRY2 inhibitors were all concomitantly downregulated only in AKT/Ras liver lesions, suggesting that their suppression is responsible for Ras/MAPK elevated activation in AKT/Ras mice. Ras might also achieve unrestrained activation via suppression of either the ephrin A2 receptor (EPHA2) or its receptor ligand, EFNA1.[26] However, we found that both EPHA2 and EFNA1 were rather upregulated in AKT/Ras liver lesions (Supplementary Fig. 9), indicating that Ras unrestrained activity does not depend on suppression of the EPHA2/EFNA1 axis in this mouse model. Thus, co-expression of N-Ras and AKT in the mouse liver reinforces Ras activity via suppression of Ras inhibitors.

DISCUSSION

Mounting evidence indicates that activation of AKT and Ras pathways is a key oncogenic event in human hepatocarcinogenesis.[3-6] However, no investigation has been previously conducted to unravel the functional crosstalk between the two cascades in HCC. Here, we used *in vivo* mouse models and *in vitro* assays to address the cellular and molecular mechanisms whereby these two oncogenic pathways promote hepatic malignant transformation and tumor progression. Our results demonstrate that co-expression of AKT and N-Ras in the mouse liver promotes rapid hepatocarcinogenesis *in vivo*, providing strong genetic evidence that combined deregulation of AKT and Ras pathways plays a pivotal role in liver cancer development. In particular, we found that the major effect of AKT and N-Ras interaction in hepatocarcinogenesis is the increase in cell proliferation and angiogenesis, leading to fast malignant transformation and tumor progression in AKT/Ras mice. No anti-apoptotic advantages were detected when comparing AKT/Ras livers with corresponding lesions from AKT mice.

In a recent study, it has been shown that AKT, when co-expressed with activated K-Ras, promotes carcinogenesis in the mouse pancreas via inhibition of Ras-induced senescence.[27] The latter pathogenetic mechanism does not seem to apply to our mouse model, since no differences in β-galactosidase staining (not shown) and in the expression of senescence markers such as $p16^{INK4A}$, $p19^{ARF}$, $P21^{CIP1}$, and p53BP1 were detected in the lesions from Ras, AKT, and AKT/Ras mice (Supplementary Fig. 10). Thus, it appears that aberrant co-activation of AKT and Ras exerts different biologic and molecular effects, depending upon the cell type and the tumor model used. Also, we cannot exclude that different Ras genes might induce distinct cellular and molecular responses in AKT-overexpressing cells. Recently, for instance, it has been shown that activated H-Ras induced senescence in F9 mouse embryonal cells, while no sign of senescence were detected in the same cell line following overexpression of either mutated Ki-Ras or oncogenic N-Ras.[28] On the other hand, both oncogenic Ki-Ras and H-Ras induced senescence in normal fibroblasts, whereas only activated H-Ras promoted senescence in osteosarcoma U2OS cells.[29] Thus, additional studies are needed to better define the pathogenetic role of each Ras gene in liver cancer.

At the molecular level, co-expression of AKT and N-Ras protooncogenes in the liver resulted in a synergistic effect leading to higher levels of mTORC1 and ERK activation. In particular, we found AKT/Ras tumors showed high mTORC1 activity via ERK-dependent phosphorylation of TSC2, in agreement with previous data from breast and colon

carcinoma.[15] Furthermore, Ras/MAPK activation was amplified in AKT/Ras tumors by suppression of Ras/MAPK inhibitors, including RASAL1, DAB2IP, NORE1A, RKIP, and SPRY2, whose inactivation has also been frequently detected in human HCC.[3,4,6] These data, together with the downregulation of the Ras/MAPK inhibitors, RASSF1A and DUSP1, by proteasome-dependent degradation, imply the existence of a complex genetic program leading to unrestrained activation of Ras/MAPK both in AKT/Ras mice (this study) and human HCC. In addition, we found that the enhancement of proliferation and angiogenesis in AKT/Ras preneoplastic and neoplastic lesions is mediated by both mTORC1-dependent and –independent mechanisms. The central role played by mTORC1 in AKT/Ras hepatocarcinogenesis is underscored by the lack of increase in the activation of mTORC2 and other pathways involved in hepatocarcinogenesis, including Jak/Stat, WNT-β-catenin, and Hedgehog (not shown) in AKT/Ras preneoplastic and neoplastic lesions. On the other hand, we found that cooperation between AKT and N-Ras resulted in the induction of growth promoting stimuli that were mTORC1-independent as well. The latter consisted of upregulation of the transcription factors FOXM1 and c-Myc, two major players in hepatocyte proliferation and tumor development.[30] Although FOXM1 and c-Myc can modulate each other's activity in various cell types,[30] the present data indicate that these two protooncogenes lie in two distinct cascades in AKT/Ras hepatocarcinogenesis. We are currently in the process of elucidating the contribution of each of these signaling pathways in mediating AKT/Ras induced hepatocarcinogenesis using animal models. These studies will provide further mechanistic insights into the genetic and biochemical interactions between Ras/MAPK and AKT/mTOR cascades in promoting liver tumor development.

mTOR inhibitors have been considered as promising new drugs in treating solid tumors, including HCC. Early phase clinical trials for Rapamycin analogs (Rapalogs), such as Everolimus are in progress.[31] However, the available data indicate a limited efficacy of Rapalogs against advanced HCC. Because of the frequent concomitant activation of Ras/MAPK and AKT/mTOR pathways in human HCC,[3-6] the simultaneous inhibition of both oncogenic cascades might be highly beneficial to improve the prognosis in these patients' subset. Since our AKT/Ras mouse model exhibits concomitant activation of AKT/mTOR and Ras/MAPK pathways, it provides an ideal system to test the efficacy of MAPK and mTOR inhibitors on HCC development and progression. Such studies will advance the knowledge of targeted therapy for HCC and provide solid preclinical evidence for utilizing MAPK and/or mTOR inhibitors in human HCC treatment. Furthermore, our preclinical model suggests co-activation of AKT and Ras signalling leads to activation of FOXM1/SKP2 and c-Myc cascades during hepatocarcinogenesis in a mTORC1-independent manner. The aberrant activation of FOXM1/SKP2 and c-Myc might confer limited efficacy and/or resistance to therapy with mTOR inhibitors in HCC. Therefore, the use of drugs that interfere with other important pathways downstream of Ras and AKT that have been identified in this study, such as the SKP2-mediated protein degradation cascade, might be helpful in combination with mTOR inhibitors for the treatment of HCC.

Supplementary Material

Refer to Web version on PubMed Central for supplementary material.

Acknowledgments

Grant support: This work was supported by NIH grants R21CA131625 and R01CA136606 to XC; P30DK026743 for UCSF Liver Center; the Deutsche Forschungsgemeinschaft DFG (grant number Do622/2-1) to FD. SM and GD were supported in part by a fellowship from the Master and Back Program, Sardegna Ricerche, RAS.

Abbreviations

AKT	v-akt murine thymoma viral oncogene homolog
FOXM1	forkhead box M1
HCC	hepatocellular carcinoma
MAPK	mitogen-activated protein kinase
mTOR	mammalian target of rapamycin
mTORC	mTOR complex
N-Ras	neuroblastoma Ras viral oncogene homolog
RAPTOR	regulatory-associated protein of mTOR
RICTOR	rapamycin-insensitive companion of mTOR
RPS6	ribosomal protein S6
TSC2	tuberin

REFERENCES

1. Bruix J, Boix L, Sala M, et al. Focus on hepatocellular carcinoma. Cancer Cell. 2004; 5:215–219. [PubMed: 15050913]
2. Spangenberg HC, Thimme R, Blum HE. Targeted therapy for hepatocellular carcinoma. Nat Rev Gastroenterol Hepatol. 2009; 6:423–432. [PubMed: 19488072]
3. Calvisi DF, Ladu S, Gorden A, et al. Ubiquitous activation of Ras and Jak/Stat pathways in human HCC. Gastroenterology. 2006; 130:1117–1128. [PubMed: 16618406]
4. Calvisi DF, Ladu S, Conner EA, et al. Inactivation of Ras GTPase-activating proteins promotes unrestrained activity of wild-type Ras in human liver cancer. J Hepatol. 2011; 54:311–319. [PubMed: 21067840]
5. Villanueva A, Chiang DY, Newell P, et al. Pivotal role of mTOR signaling in hepatocellular carcinoma. Gastroenterology. 2008; 135:1972–1983. [PubMed: 18929564]
6. Calvisi DF, Ladu S, Gorden A, et al. Mechanistic and prognostic significance of aberrant methylation in the molecular pathogenesis of human hepatocellular carcinoma. J Clin Invest. 2007; 117:2713–2722. [PubMed: 17717605]
7. Schubbert S, Shannon K, Bollag G. Hyperactive *Ras* in developmental disorders and cancer. Nat Rev Cancer. 2007; 7:295–308. [PubMed: 17384584]
8. Vivanco I, Sawyers CL. The phosphatidylinositol 3-Kinase AKT pathway in human cancer. Nat Rev Cancer. 2002; 2:489–501. [PubMed: 12094235]
9. Zoncu R, Efeyan A, Sabatini DM. mTOR: from growth signal integration to cancer, diabetes and ageing. Nat Rev Mol Cell Biol. 2011; 12:21–35. [PubMed: 21157483]
10. Lee SA, Ho C, Roy R, et al. Integration of genomic analysis and in vivo transfection to identify sprouty 2 as a candidate tumor suppressor in liver cancer. Hepatology. 2008; 47:1200–1210. [PubMed: 18214995]
11. Carlson CM, Frandsen JL, Kirchhof N, et al. Somatic integration of an oncogene-harboring Sleeping Beauty transposon models liver tumor development in the mouse. Proc Natl Acad Sci U S A. 2005; 102:17059–17064. [PubMed: 16286660]
12. Calvisi DF, Wang C, Ho C, et al. Increased lipogenesis, induced by AKT-mTORC1-RPS6 signaling, promotes development of human hepatocellular carcinoma. Gastroenterology. 2011; 140:1071–1083. [PubMed: 21147110]
13. Frith CH, Ward JM, Turusov VS. Tumours of the liver. IARC Sci Publ. 1994; 111:223–269. [PubMed: 8082908]
14. Xu CR, Lee S, Ho C, et al. Bmi1 functions as an oncogene independent of Ink4A/Arf repression in hepatic carcinogenesis. Mol Cancer Res. 2009; 7:1937–1945. [PubMed: 19934271]

15. Ma L, Chen Z, Erdjument-Bromage H, Tempst P, Pandolfi PP. Phosphorylation and functional inactivation of TSC2 by Erk implications for tuberous sclerosis and cancer pathogenesis. Cell. 2005; 121:179–193. [PubMed: 15851026]
16. Manning BD, Tee AR, Logsdon MN, et al. Identification of the tuberous sclerosis complex-2 tumor suppressor gene product tuberin as a target of the phosphoinositide 3-kinase/akt pathway. Mol Cell. 2002; 10:151–162. [PubMed: 12150915]
17. Sancak Y, Thoreen CC, Peterson TR, et al. PRAS40 is an insulin-regulated inhibitor of the mTORC1 protein kinase. Mol Cell. 2007; 25:903–915. [PubMed: 17386266]
18. Karni R, Hippo Y, Lowe SW, et al. The splicing-factor oncoprotein SF2/ASF activates mTORC1. Proc Natl Acad Sci U S A. 2008; 105:15323–15327. [PubMed: 18832178]
19. Carrière A, Cargnello M, Julien LA, et al. Oncogenic MAPK signaling stimulates mTORC1 activity by promoting RSK-mediated raptor phosphorylation. Curr Biol. 2008; 18:1269–1277. [PubMed: 18722121]
20. Wang IC, Chen YJ, Hughes D, et al. Forkhead box M1 regulates the transcriptional network of genes essential for mitotic progression and genes encoding the SCF (Skp2-Cks1) ubiquitin ligase. Mol Cell Biol. 2005; 25:10875–10894. [PubMed: 16314512]
21. Frescas D, Pagano M. Deregulated proteolysis by the F-box proteins SKP2 and beta-TrCP: tipping the scales of cancer. Nat Rev Cancer. 2008; 8:438–449. [PubMed: 18500245]
22. Song MS, Song SJ, Kim SJ, et al. Skp2 regulates the antiproliferative function of the tumor suppressor RASSF1A via ubiquitin-mediated degradation at the G1-S transition. Oncogene. 2008; 27:3176–3185. [PubMed: 18071316]
23. Lin YW, Yang JL. Cooperation of ERK and SCFSkp2 for MKP-1 destruction provides a positive feedback regulation of proliferating signaling. J Biol Chem. 2006; 281:915–26. [PubMed: 16286470]
24. Zhu J, Blenis J, Yuan J. Activation of PI3K/Akt and MAPK pathways regulates Myc-mediated transcription by phosphorylating and promoting the degradation of MAD1. Proc Natl Acad Sci U S A. 2008; 105:6584–6589. [PubMed: 18451027]
25. Zimmermann S, Moelling K. Phosphorylation and regulation of Raf by Akt (protein kinase B). Science. 1999; 286:1741–1744. [PubMed: 10576742]
26. Macrae M, Neve RM, Rodriguez-Viciana P, et al. A conditional feedback loop regulates Ras activity through EphA2. Cancer Cell. 2005; 8:111–118. [PubMed: 16098464]
27. Kennedy AL, Morton JP, Manoharan I, et al. Activation of the PIK3CA/AKT pathway suppresses senescence induced by an activated RAS oncogene to promote tumorigenesis. Mol Cell. 2011; 42:36–49. [PubMed: 21474066]
28. Quinlan MP, Quatela SE, Philips MR, Settleman J. Activated Kras, but not Hras or Nras, may initiate tumors of endodermal origin via stem cell expansion. Mol Cell Biol. 2008; 28:2659–2674. [PubMed: 18268007]
29. Bihani T, Mason DX, Jackson TJ, Chen SC, Boettner B, Lin AW. Differential oncogenic Ras signaling and senescence in tumor cells. Cell Cycle. 2004; 3:1201–1207. [PubMed: 15492501]
30. Costa RH, Kalinichenko VV, Holterman AX, et al. Transcription factors in liver development, differentiation, and regeneration. Hepatology. 2003; 38:1331–1347. [PubMed: 14647040]
31. Whittaker S, Marais R, Zhu AX. The role of signaling pathways in the development and treatment of hepatocellular carcinoma. Oncogene. 2010; 29:4989–5005. [PubMed: 20639898]

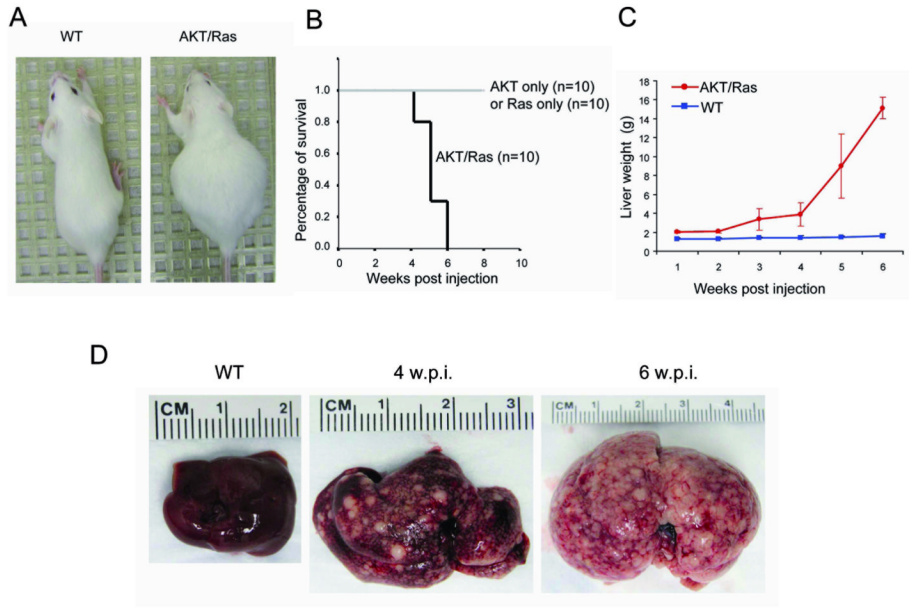

Figure 1.

Co-expression of myristylated AKT1 (myr-AKT) and mutated N-Ras (N-RasV12) induces mouse liver tumor development. (A) Phenotype of the wild-type (WT) and AKT/Ras mouse (4 weeks post injection). (B) Survival curve of AKT only, Ras only, and AKT combined with Ras injected mice. (C) Liver weight of wild-type and AKT/Ras mice at different time points (1 to 6 weeks post injection). (D) Gross images of wild-type (WT) liver and AKT/Ras mice livers 4 or 6 weeks post injection (w.p.i).

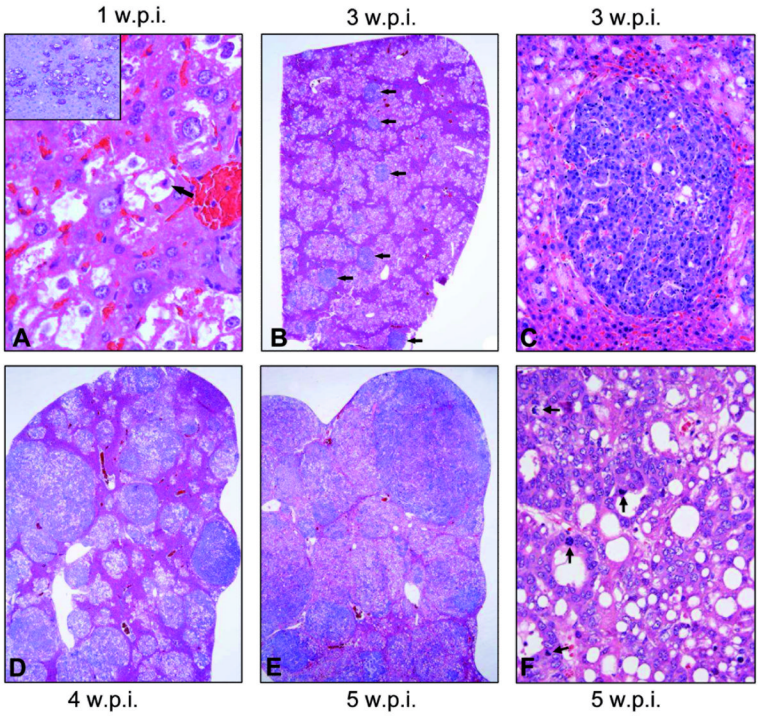

Figure 2.

Stepwise hepatocarcinogenesis in AKT/Ras mice. Three weeks after injection already about 60% of the liver tissue was occupied by lesions (*A*). The latter were mostly consisting of preneoplastic hepatocytes, that began to emerge few days after injection (higher magnification in *A* with arrow on mitosis; one week after injection), and were characterized by a clear cytoplasm due to an increase in fat and glycogen-storing (glycogen staining in the PAS reaction; *inset*). At this stage, the first small hepatocellular adenomas originated from the clear cell foci (arrows in *B*; higher magnification in *C*). (*D*) Four weeks after injection, many of these tumors have grown to a size of several millimeters in diameter, replacing much of the former preneoplastic and normal liver tissue. (*E*) Five weeks after injection, many tumors further progressed to frankly malignant neoplasms that have replaced most of the normal liver tissue. (*F*) Typical example of a hepatocellular carcinoma. Tumors often showed a mixed phenotype with dominating hepatocellular differentiation, trabecular growth intermingled with ductular/pseudoglandular areas and a lesser degree of fat storage than in preneoplasias. Several mitotic figures are indicated by arrows. All H&E staining, except for the inset (PAS reaction). The lower edge of the panel represents 0.3 mm in *A*, 0.5 mm in inset, 4.9 mm in *B*,*D*,*E*, 0.7 mm in *C*, and 0.3 mm in *F*.

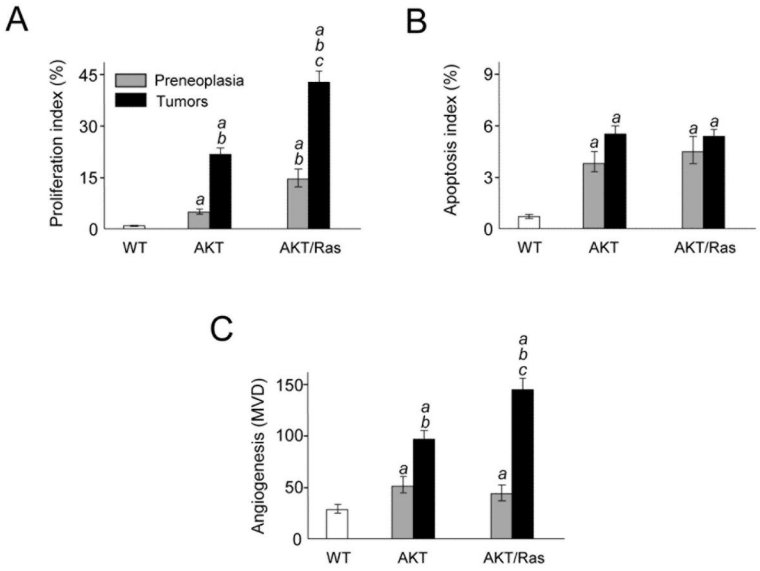

Figure 3.

Proliferation (*A*), apoptosis (*B*), and angiogenesis (*C*; microvessel density, MVD) indices in wild-type livers and preneoplastic and neoplastic livers developed in AKT and AKT/Ras mice. Ten samples per each group per each assay were analyzed. Each *bar* represents mean ± SD. Tukey-Kramer test: $P < 0.0001$ *a*, *vs*. wild-type liver; *b*, *vs*. AKT preneoplastic liver; *c*, *vs.* AKT tumors.

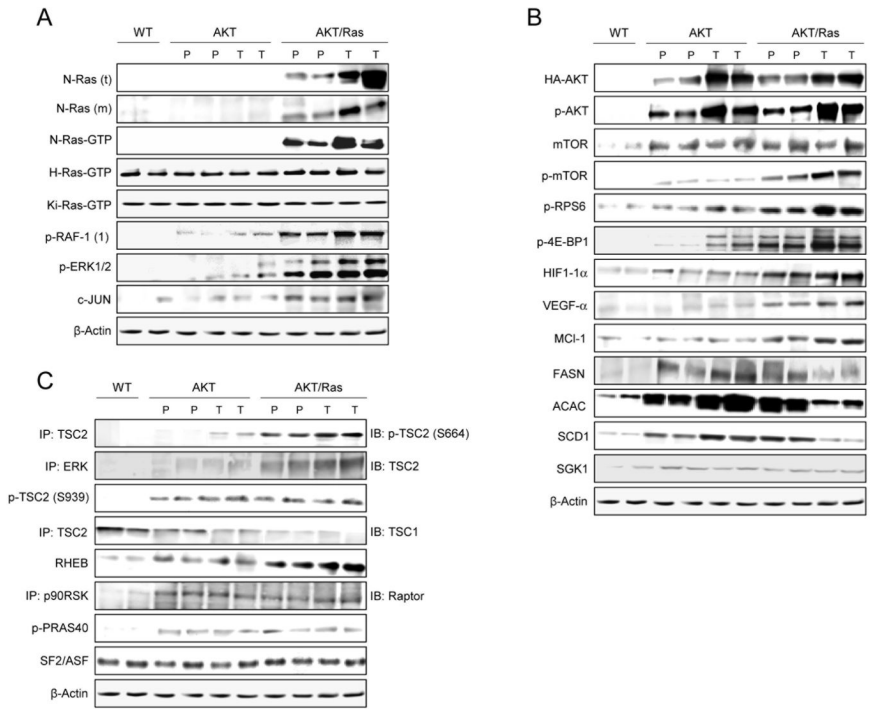

Figure 4.

Levels of activation of N-Ras/MAPK, mTORC1, and mTORC2 pathways in wild-type, AKT, and AKT/Ras mice. (*A*) Representative immunoblotting of the Ras proteins and their major downstream effectors. Both total (t) and membranous (m; sign of activation) levels of N-Ras were determined. Levels of activated (Ras-GTP) N-Ras, H-Ras, and Ki-Ras were assessed. The abbreviation p-RAF-1(1) indicates phosphorylation/activation of RAF-1 at serine 338 by Ras. (*B*) Representative immunoblotting of AKT, mTOR and their downstream effectors in the mTORC1 (p-RPS6, p-4E-BP1, HIF-1α, VEGF-α, MCL-1, FASN, ACAC, SCD1) and mTORC2 (LIPIN1, SGK1) complexes. (*C*) Assessment of TSC2 regulators by immunoblotting. Six to nine samples per each group per each assay were analyzed. Expression patterns for the same proteins did not show significant difference between wild-type and N-Ras injected livers (not shown). Abbreviations: IB, immunoblotting; IP, immunoprecipitation; WT, wild-type; P, preneoplasia; T, tumor.

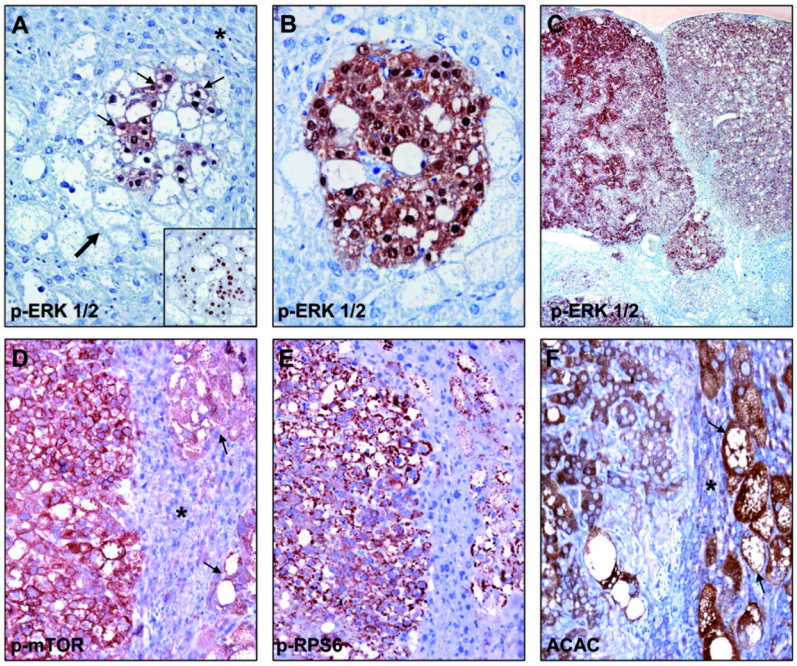

Figure 5.

(*A*) Appearance of a subset of small cells (thin arrows) within clear-cell preneoplastic lesions (thick arrow) surrounded by normal liver tissue (asterisk) exhibiting strong phosphorylation/activation of ERK proteins (p-ERK1/2) during AKT/Ras neoplastic transformation. These cells are characterized by a high proliferation rate (inset). Maintenance of p-ERK1/2 overexpression in a resulting small tumor (*B*) and in subsequent, large hepatocellular carcinomas (*C*). (*D*,*E*) Immunohistochemical staining for phosphorylated/activated mTOR (p-mTOR) and its target phosphorylated/activated RPS6 (p-RPS6) in serial sections, showing a HCC (left part), preneoplasias (arrows in *D*) and surrounding normal liver tissue (marked in *D* with an asterisk). (*F*) Overexpression of the lipogenic enzyme ACAC in the same mouse sample: HCC (left), preneoplastic cells (arrows) and normal tissue (asterisk). Note the strongest staining for p-mTOR and p-RPS6 in HCC and in preneoplastic liver for ACAC, respectively. The lower edge of the panel represents 0.4 mm in *A*, 0.3 mm in *B*, 2.5 mm in *C*, 0.5 mm in *D*-*F*.

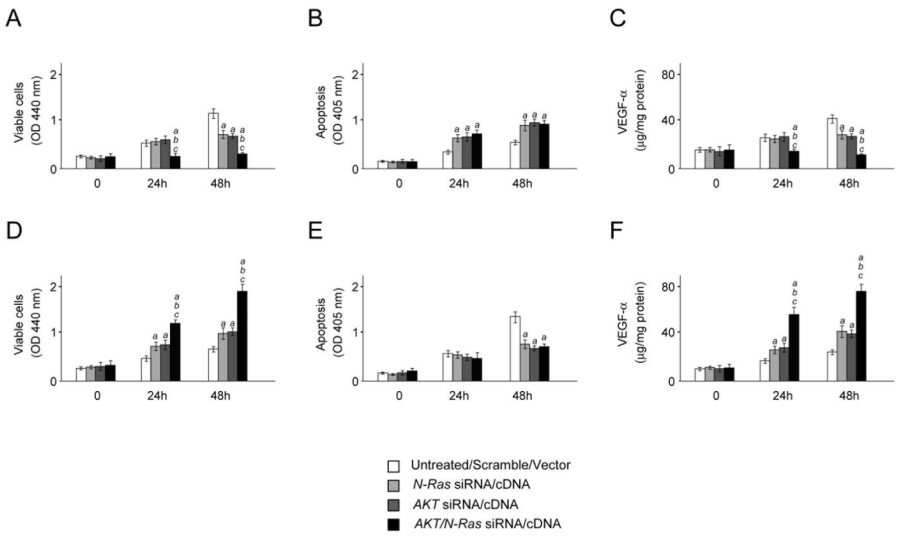

Figure 6.

(*A-C*) Effect of suppressing AKT and N-Ras, either alone or in combination, via siRNA on cell viability (A), apoptosis (B), and angiogenesis (C; assessed by VEGF-α secretion in the medium) in the AKT/Ras cell line. Equivalent results were obtained in SNU-389 cells (not shown). (*D-F*) Effect of overexpressing *AKT* and N-Ras, either alone or in combination, via transient transfection on cell viability (*D*), apoptosis (*E*), and angiogenesis (*F*; assessed by VEGF-α secretion in the medium) in the human HLF HCC cell line. Cells were maintained as monolayer cultures in DMEM supplemented with 10% fetal bovine serum, serum-starved for 24 h, and then treated with either specific siRNAs or respective cDNAs. Results at 24 and 48 hours are shown. Each bar represents mean ± SD of 3 independent experiments conducted in triplicate. Results from untreated and scramble treated cells did not differ significantly and are, thus, merged. Tukey-Kramer test: $P < 0.0001$ *a*, vs. control (untreated cells); *b*, vs. *N-Ras* siRNA/cDNA; *c*, *vs. AKT* siRNA/cDNA.

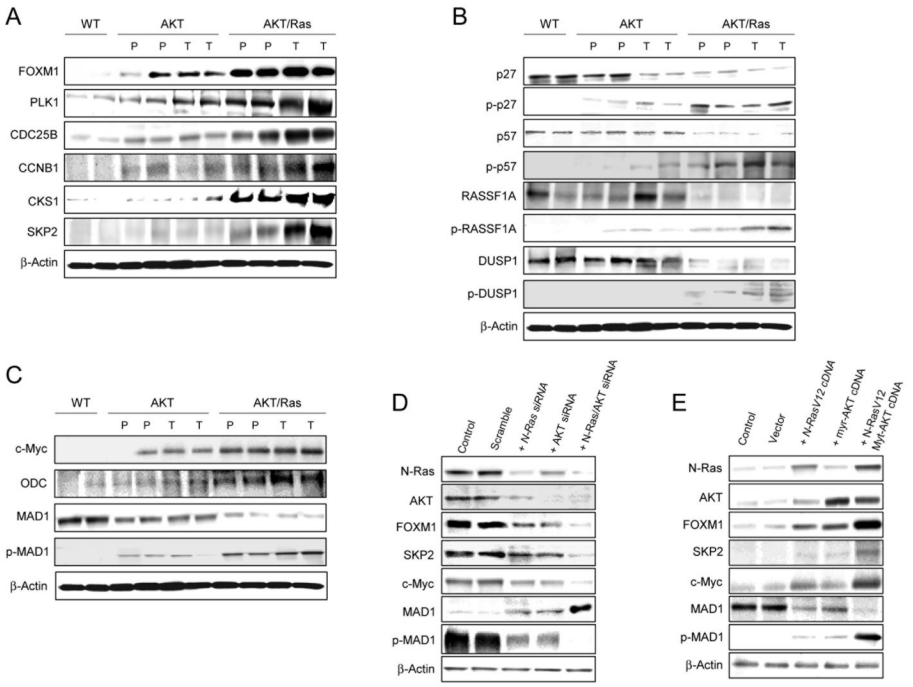

Figure 7.

Activation of FOXM1 and c-Myc pathways in AKT/Ras tumors. (*A*) Levels of FOXM1 and its targets in wild-type, AKT, and AKT/Ras mice as assessed by immunoblotting. (*B*) Representative immunoblotting of the proteins targeted to SKP2-dependent ubiquitination following phosphorylation at specific sites. (*C*) Levels of c-Myc and its targets as assessed by immunoblotting. Expression patterns for the same proteins did not show significant difference between wild-type and N-Ras injected livers (not shown). Abbreviations: WT, wild-type; P, preneoplasia; T, tumor. (*D*) Effect of suppressing *N-Ras* and *AKT*, either alone or in combination, via siRNA on the levels of FOXM1 and c-Myc pathways in the AKT/Ras cell line. Equivalent results were obtained in SNU-389 cells (not shown). (*E*) Effect of overexpressing *Ras* and *AKT*, either alone or in combination, via transient transfection on the levels of FOXM1 and c-Myc pathways in the human HLF HCC cell line. Cells were maintained as monolayer cultures in DMEM supplemented with 10% fetal bovine serum, serum-starved for 24 h, and then transfected with either specific siRNAs or respective cDNAs. Results at 48 hours are shown.

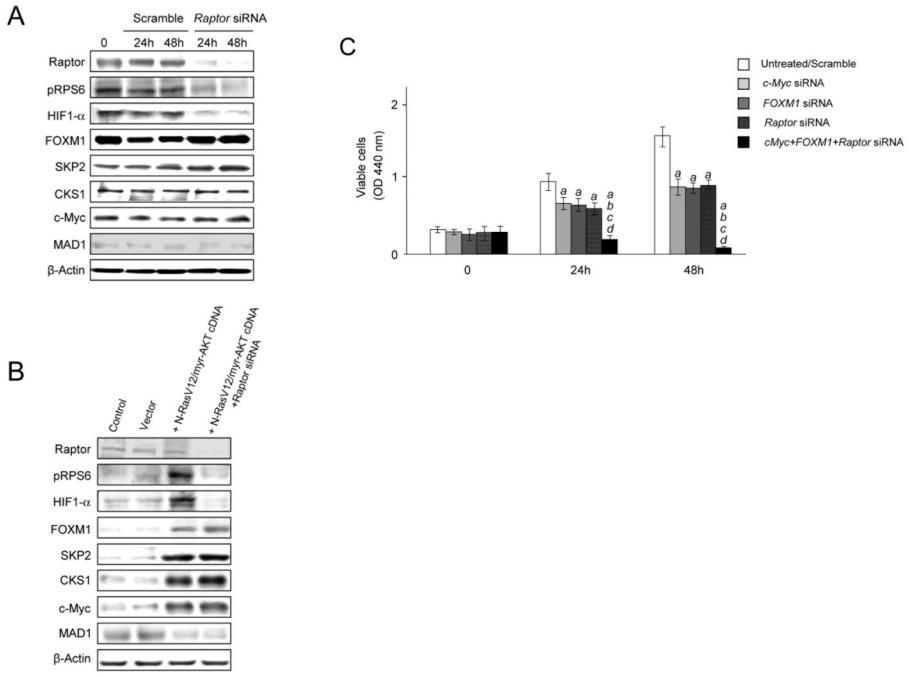

Figure 8.

(*A*) Effect of suppressing Raptor via specific siRNA on the levels of mTORC1 (p-RPS6, HIF-1α), FOXM1 (FOXM1, SKP2, CKS1), and c-Myc (c-Myc, MAD1) targets in the AKT/Ras cell line. (*B*) Effect of co-expressing myristylated AKT (myr-AKT) and mutated N-Ras (N-RasV12) either alone or in combination with Raptor silencing on the levels of mTORC1 (p-RPS6, HIF-1α), FOXM1 (FOXM1, SKP2, CKS1), and c-Myc (c-Myc, MAD1) targets in the HLF cell line. (*C*) Effect of suppressing c-Myc and FOXM1 genes either alone or together with Raptor silencing via specific siRNAs in the AKT/Ras cell line. Cells were maintained as monolayer cultures in DMEM supplemented with 10% fetal bovine serum, serum-starved for 24 h, and then treated with either specific siRNAs or respective cDNAs. Results at 24 and 48 hours are shown. Each bar represents mean ± SD of 3 independent experiments conducted in triplicate. Results from untreated and scramble treated cells did not differ significantly and are, thus, merged. Tukey-Kramer test: $P < 0.0001$ *a*, vs. control (untreated cells); *b*, vs. *c-Myc* siRNA; *c*, *vs. FOXM1*-siRNA; *d*, vs. *Raptor* siRNA.